



OPEN

## CVRmap—a complete cerebrovascular reactivity mapping post-processing BIDS toolbox

A. Rovai<sup>1,2</sup>✉, V. Lolli<sup>3,4</sup>, N. Trotta<sup>1,2</sup>, S. Goldman<sup>1</sup> & X. De Tiège<sup>1,2</sup>

Cerebrovascular Reactivity (CVR) refers to the ability of cerebral blood vessels to dilate or constrict under the effect of vasoactive substances and can be estimated using functional Magnetic Resonance Imaging (fMRI). Computation of CVR maps is relevant in various brain diseases and requires specialized data processing. We introduce CVRmap, an opensource software that automates the computation of CVR map. The toolbox complies with the Brain Imaging Data Structure (BIDS) standards.

Cerebro-Vascular Reactivity (CVR) quantifies the ability of cerebral vessels to dilate or constrict under the effect of vasoactive substances such as the blood CO<sub>2</sub> partial pressure. It can be estimated using functional Magnetic Resonance Imaging (fMRI) since the Blood Oxygen Level Dependent (BOLD) signal is a surrogate for local blood flow<sup>1–3</sup>, and blood CO<sub>2</sub> partial pressure can be altered using breathing challenges such as CO<sub>2</sub> inhalation<sup>4</sup>, breath-hold<sup>5</sup>, progressive hypercapnia<sup>6</sup>, end-tidal CO<sub>2</sub> forcing<sup>7</sup> or even resting-state<sup>8</sup>. The relative change in the BOLD signal is then divided by the change in CO<sub>2</sub> blood partial pressure to obtain CVR<sup>9,10</sup>. CVR can be used to assess vascular integrity and has a growing range of clinical applications<sup>11,12</sup>. In most studies using CVR, preprocessing and CVR mapping is done using in-house scripts, posing several problems regarding results reproducibility and methodological transparency. Moreover, there are no openly accessible datasets on which CVR methods can be experienced, tested, or compared.

### Main

This work aims to fill these gaps by offering to the community a standard framework for the computation of CVR in a variety of research topic, whether in clinical or more neuroscience-oriented projects, as well as an openly accessible normative dataset. CVRmap complies with the Brain Imaging Data Structure (BIDS)<sup>13</sup> standards for data processing applications. It works hand-in-hand with preprocessed data from fMRIPrep<sup>14</sup> but could also be used with other conventional preprocessing pipelines provided the BIDS layout is respected. With this effort, we push the field to be part of the openscience culture, fostering the transparency of the methods, collaborative work and data sharing.

Imaging data must be accompanied by recordings of breath CO<sub>2</sub> concentration and converted into a BIDS-compliant dataset as described in the BIDS documentation. The user can launch the CVRmap pipeline after preprocessing by fMRIPrep. There is no other requirement on the data structure, making the stream stable and easy to use. The pipeline checks that the provided data matches the expected inputs and produces readable error messages if the dataset is not suitable for CVR analysis.

The pipeline is agnostic of the experimental paradigm: the mathematics used to model the BOLD signal and estimate CVR<sup>9</sup> holds irrespective to the breathing challenge. Researchers can therefore analyze their data from different protocols using the same exact tool, allowing a reliable comparison of the results.

The first step is to estimate the CO<sub>2</sub> blood partial pressure timecourse from the breathing CO<sub>2</sub> recordings. A faithful proxy of blood CO<sub>2</sub> is the end-tidal CO<sub>2</sub> (etCO<sub>2</sub>), which corresponds to the upper envelope of the breathing data. The pipeline performs this physiological data preprocessing step automatically, removing breathing patterns and taking care of potential noise sources by smoothing the timecourse. These steps are compatible with virtually any CO<sub>2</sub>-recording device, in particular, the pipeline accommodates for any sampling frequency.

<sup>1</sup>Université Libre de Bruxelles (ULB), ULB Neuroscience Institute (UNI), Laboratoire de Neuroanatomie et de Neuroimagerie translationnelles, Université libre de Bruxelles, Brussels, Belgium. <sup>2</sup>Université Libre de Bruxelles (ULB), Hôpital Universitaire de Bruxelles (HUB), CUB Hôpital Erasme, Department of Translational Neuroimaging, Université Libre de Bruxelles, Brussels, Belgium. <sup>3</sup>Université Libre de Bruxelles (ULB), Hôpital Universitaire de Bruxelles (HUB), Hôpital des Enfants Reine Fabiola, Department of Radiology, Université Libre de Bruxelles, Brussels, Belgium. <sup>4</sup>Université Libre de Bruxelles (ULB), Hôpital Universitaire de Bruxelles (HUB), CUB Hôpital Erasme, Department of Radiology, Université Libre de Bruxelles, Brussels, Belgium. ✉email: antonin.rovai@hubruxelles.be

The second step is to denoise the fMRI data using the fMRIPrep outputs which includes Independent Component Analysis (ICA)-based strategy for Automatic Removal of Motion Artefacts (ICA-AROMA<sup>15</sup>). CVRmap uses a refinement of the ICA-AROMA classification to ensure that noisy Independent Component (IC) do not share resemblance with the CO<sub>2</sub> proxy<sup>16</sup>. This re-selection of noise ICs is necessary to ensure that physiological signal of interest is not removed from the data. The non-aggressively denoised data emerging from this procedure are automatically computed<sup>15</sup>.

The final step deals with time delays expected between etCO<sub>2</sub> and BOLD signal. The pipeline takes care of local time delays on a voxel-by-voxel basis by systematically exploring time shifts between etCO<sub>2</sub> and BOLD signals<sup>17–20</sup>. This shift-and-search procedure implies a robust extrapolation of the etCO<sub>2</sub> curve without the necessity of trimming the original BOLD signal. The results are summarized on delay maps, the time of reference being set to the global BOLD signal. The BOLD signal is modeled using the optimally shifted etCO<sub>2</sub> at each voxel<sup>9</sup>:

$$\text{BOLD} = \beta_0 + \beta_1 \times \text{shifted-etCO}_2,$$

where  $\beta_0$  and  $\beta_1$  are fitted parameters at optimal time-shifts, from which CVR is computed by

$$\text{CVR} = \frac{\beta_1}{\beta_0 + \beta_1 \times \text{etCO}_2\text{-baseline}}.$$

All these steps of the pipeline are summarized on the workflow diagram on Fig. 1.

Users have access to all intermediate steps and final results of the pipeline through easy-to-read and share visual reports for each participant. It includes original and preprocessed physiological and global BOLD signal timecourses for quality check purposes and present a summary of the noise-IC re-selection process. CVR and maps of optimal delay are presented using mosaic layouts. The report, being written in HTML, can be opened in any web-browser.

CVR and delay maps are saved in accordance with the BIDS derivatives standard as compressed NIFTI files in either participant or Montreal Neurological Institute (MNI) template space. The former is useful for patients, whose anatomical abnormalities may compromise the quality of the normalization to template space, and can be directly coregistered and overlaid with original anatomical scans. Maps in template space, derived from the sophisticated outputs of fMRIPrep, can be used to perform group-level analysis. CVRmap is limited to participant-level processing, but the easy and intuitive layout of the outputs, following the guidelines of the BIDS for derived data, makes it easy to incorporate the individual results into custom group-level analysis pipelines or any other region-of-interest analysis.

The pipeline was validated on a cohort of 50 healthy adults (25 females, mean age: 33.6 y, age range 21–67 y) who underwent an fMRI session with hypercapnic blocs following the protocol of<sup>4</sup>. CVRmap finished without errors on the whole dataset. Mean CVR was computed in gray matter (GM) and white matter (WM) and grouped in three age categories (less than 30 y, between 30y and 50 y, and more than 50 y). The results are presented on Fig. 2, and show a higher CVR in GM than in WM for each age group and a decrease of CVR with age (in agreement with the data from the literature<sup>10,21</sup>). We also show mean CVR maps in axial plane in MNI space, obtained by fitting a General Linear Model with the age of the participant as a regressor to extract age-corrected data. The dataset is shared online, allowing researchers to perform quantitative comparison between their data and this normative dataset.

## Methods

CVRmap is an opensource software that computes maps of Cerebro-Vascular Reactivity from fMRI data recorded alongside continuous breathing CO<sub>2</sub> measurements. It is developed in the powerful framework of the BIDS<sup>13</sup>, in particular taking advantage of the robust preprocessing tool fMRIPrep<sup>22</sup>. CVRmap has various installation solutions including containerized environments, which makes it easy to use by clinicians or researchers without advanced skills in programming. More specifically, basic knowledge of the command-line in Unix-like environment is the only prerequisite to use CVRmap. It runs mostly automatically, and yet can be adapted to the user's specific needs owing to several run options such as participant label, target space, task name, denoising strategy, fMRIPrep and output directory. More specific needs can also be satisfied by specifying a custom configuration file to tune the parameters such as spatial or temporal smoothing strength. The processing for a single participant takes about 15 min to complete on a standard workstation (4 Gb of memory, Intel Core i7, using one thread). The comprehensive reports allow for a quick and efficient visual overview of the results. We refer to Fig. 3 for an example of such report.

The pipeline is agnostic of the experimental paradigm. For any breathing challenge allowing continuous monitoring of breathing CO<sub>2</sub>, e.g. CO<sub>2</sub> inhalation, progressive hypercapnia<sup>6</sup>, or using end-tidal CO<sub>2</sub> forcing devices<sup>7</sup>, the mathematics implemented in CVRmap and used to model the BOLD signal to eventually estimate CVR hold<sup>9,23</sup>. Researchers can therefore analyze their data from different protocols using the same exact tool, allowing a reliable comparison of the results. Moreover, the code is shared using a standard version-control system, giving full access to previous releases or single contributions to the package. It is also open to further contribution, possibly enlarging its field of applications.

## Input data

*fMRI data.* The rigidity of the BIDS standard allows the pipeline to adapt to different types of input data, such as sessions, runs, or custom acquisition labels. The raw BOLD series itself is not mandatory, since CVRmap works on data preprocessed by fMRIPrep. The only condition is that fMRIPrep produced ICA-AROMA classification of noise sources. CVR maps can be computed for any available space in the fMRIPrep derivatives, including

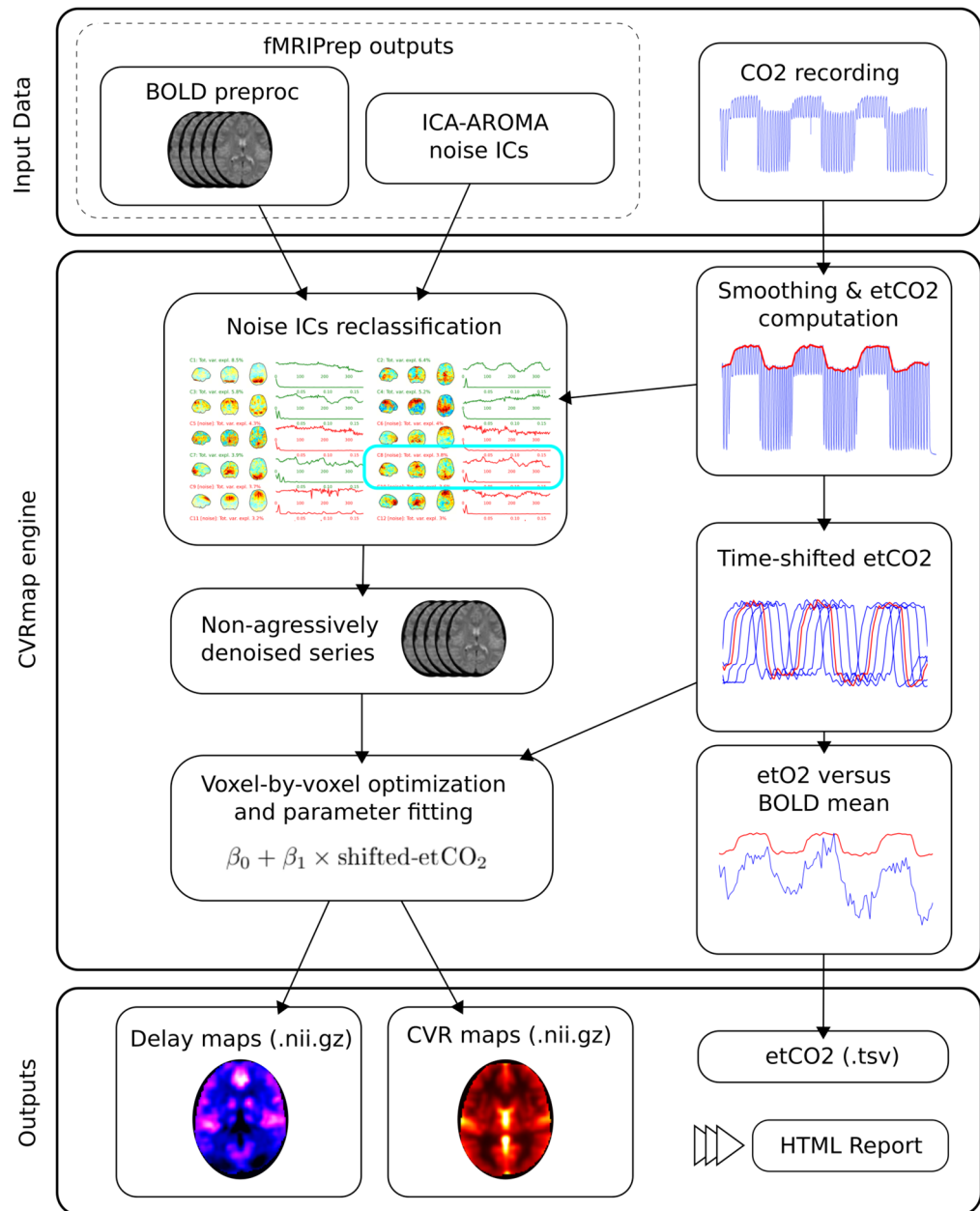


**Figure 1.** Overview of the CVRmap workflow. CVRmap runs on data preprocessed with fMRIPrep together with raw CO<sub>2</sub> readings. The end-tidal CO<sub>2</sub> timecourse is computed after a light smoothing. The noise sources as classified by ICA-AROMA are compared to the etCO<sub>2</sub> to ensure physiological signal of interest is not removed from the BOLD signal. The non-aggressively denoised data are then modeled with various time-shifted version of the etCO<sub>2</sub> timecourse to determine optimum delay and compute CVR from the fitted parameters. The pipeline saves delay and CVR maps, etCO<sub>2</sub> timecourse and a summary HTML report including control checkpoints.

participant's space. By default, CVRmap will load any series matching the 'gas' taskname, but this can be customized to meet user's needs.

Note that the details of the acquisition of the BOLD data, such as slice ordering or options like single-echo, multi-echo or multiband Echo Planar Imaging (EPI), are handled by fMRIPrep. In particular, preprocessing steps like slice-timing and realignment are automatically performed, setting the outputs of fMRIPrep on an equal footing for each of these acquisition schemes. Multi-echo EPI, whose relevance in the context of breath-hold CVR has been discussed in<sup>16,24,25</sup>, is automatically processed using the current state-of-the-art multi-echo denoising software *tedana*<sup>26</sup> within fMRIPrep. For these reasons, CVRmap itself should be blind to these details and should run equally well for data acquired using any of these techniques.

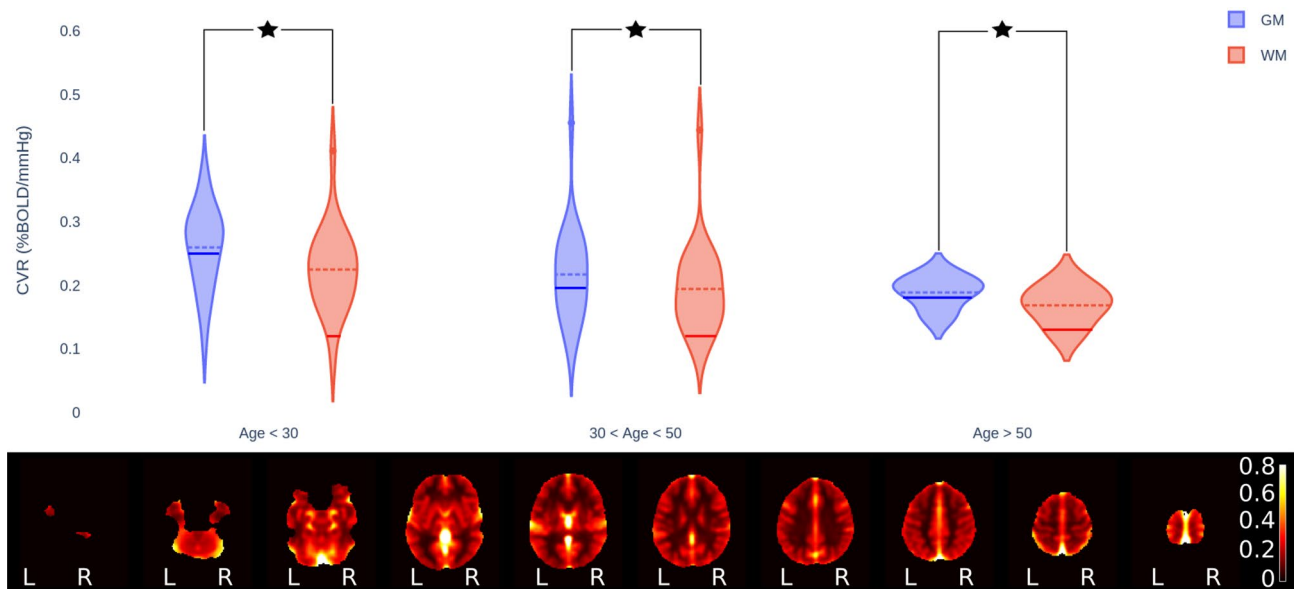


**Figure 2.** Results for the normative dataset. *Violin plots:* mean CVR for gray matter (GM) and white matter (WM), grouped by age. Dashed lines represent the mean of each distribution. Solid lines correspond to values found in the literature: for GM, it is taken from the previous study analyzing GM CVR decade-by-decade<sup>21</sup> and for WM it is taken from<sup>10</sup>. A star indicates statistical significance at  $p$ -value less than 5% for the corresponding paired  $t$ -tests. *Mosaic view of axial slices:* dataset mean of CVR maps in template (MNI) space, corrected for age (units are %BOLD/mmHg). Displayed using the neurological convention.

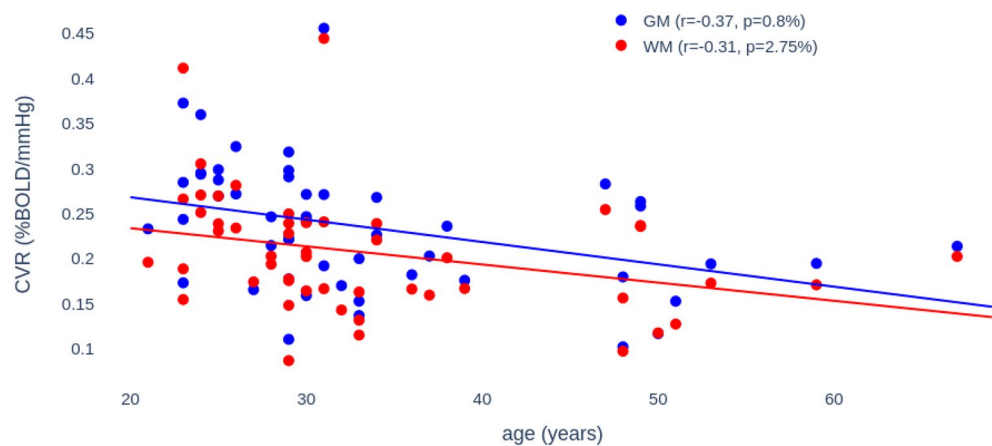


**Figure 3.** Individual Reports are produced for each participant. The reports are saved in html format. Sections include a summary of the job and the following control checkpoints: recorded physiological data versus upper envelope (etCO<sub>2</sub>), Global BOLD signal versus etCO<sub>2</sub> for alignment verification, and a representative set of axial slices, using neurological convention, of the delay and CVR maps. The report ends with a summary of the noise-IC re-classification described in the main text. Report structure has been reformatted for visual purposes.

*Physiological data.* Continuous recording of breath CO<sub>2</sub> must be included in the dataset, using the file naming scheme imposed by the BIDS and matching the BOLD task entity. The metadata file must contain the CO<sub>2</sub> sampling frequency and corresponding units. The pipeline will adapt any time-domain processing to any sampling frequency, ensuring compatibility with CO<sub>2</sub> acquisition parameters. It includes consistency checks of the input data and produces readable error messages if the dataset is not suitable for CVR processing. More specifically, CVRmap checks that the BIDS dataset contains the required preprocessed data from fMRIPrep as well as the physiological recordings associated with the selected task name. If the breathing recording is shorter in duration than the BOLD data, the associated etCO<sub>2</sub> trace is padded using a baseline interpolation. Further checks require visual inspection of the report (for instance for alignment verification between etCO<sub>2</sub> and global BOLD signal).

### Physiological data preprocessing and quality check

Recordings of CO<sub>2</sub> typically include uninteresting breathing patterns. A reliable proxy of blood CO<sub>2</sub> partial pressure is the etCO<sub>2</sub>, which corresponds to the upper envelope of the breathing data. The pipeline performs this physiological data preprocessing step automatically, removing breathing patterns and taking care of potential noise contributions by smoothing the timecourse. The result is saved together with summary plots that can be used for quality check or illustrative purposes.

### Custom BOLD denoising

fMRI data are non-aggressively denoised within CVRmap using a refined version of the ICs-based classification of motion artefact ICA-AROMA<sup>15</sup>. The original classification is known to be suited for resting-state, task, or event-based paradigms, in which physiological sources of signal are considered to be noise. In the context of CVR mapping, this is not appropriate because CVR is of physiological origin<sup>16</sup>. To solve this, CVRmap automatically computes the linear correlation between the etCO<sub>2</sub> timecourse and each noise ICs found by ICA-AROMA. Using an empirical threshold (the default value is set to 0.6, which is conventionally considered to be a moderate correlation. This can be changed by the user) on the computed correlation coefficient, CVRmap decides whether the IC should remain classified as noise or not. Based on this new classification, the denoised BOLD series are computed using the non-aggressive denoising scheme. The user can optionally adjust the threshold manually or even skip this step overall.

### Delay optimization and CVR processing

An important feature of CVR estimation is to include time delays in the analysis, which are of two types<sup>5,10,27</sup>:

1. *Global delay*: depending on the experimental setup, the CO<sub>2</sub> concentration can be recorded with a delay with respect to the BOLD series. This delay depends for instance on the length of the sampling line extending from the participant's mouth to the capnograph, typically located outside of the scanning room.
2. *Local delays*: the fluctuations of blood CO<sub>2</sub> will not reach all brain regions simultaneously. As a consequence, the BOLD response cannot be expected to be synchronous in all brain regions.

CVRmap solves both these problems by computing time-shifted versions of the etCO<sub>2</sub> timecourses<sup>28</sup>. This procedure implies a robust baseline extrapolation of the etCO<sub>2</sub> curve without the necessity of trimming the original BOLD signal. The reference delay is set to the time-shift maximizing the correlation with the whole-brain BOLD mean signal. With this choice, any global delay from different experimental protocols is effectively eliminated, and does not rely on brain segmentation or parcellation. To find local delays, CVRmap finds the optimum time-shift by modeling the BOLD signal as a general linear model (GLM) at each voxel as  $Y = \beta_0 + \beta_1 \times \text{shifted-etCO}_2$ , saving the fitted parameters of the GLM at optimal time shift<sup>28</sup>. As a by-product of this procedure the pipeline computes CVR voxelwise using<sup>9,23</sup>

$$\text{CVR} = \frac{\beta_1}{\beta_0 + \beta_1 \times \text{etCO}_2\text{-baseline}},$$

using the estimated parameters  $\beta_0$  and  $\beta_1$  at optimal time-shift.

### Output maps

CVR and delay maps are saved in the space selected by the user and in accordance with the BIDS derivatives standard as compressed NIFTI files, allowing any researcher to use them for region-of-interest or statistical group analysis. Maps in participant space are particularly useful for patients, whose potential anatomical abnormalities can compromise the quality of the normalization to template space. They can be directly overlaid with original anatomical scans. CVRmap is limited to participant-level processing, but the easy and intuitive layout of the outputs, following the guidelines of the BIDS for derived data, makes it easy to incorporate the individual results into in-house pipelines.

### CVRmap report

Users have access to all intermediate steps and a summary of the final results of the pipeline through easy-to-read and share visual reports for each participant. It includes original and preprocessed physiological and global BOLD signal timecourses for quality check purposes and present a summary of the noise-IC re-selection process. CVR and maps of optimal delay are presented as mosaics of representative axial slices. The report, being written in HTML, can be opened in any web-browser and straightforwardly shared between peers or directly uploaded online.

### Open dataset and validation

The pipeline was validated on a cohort of 50 healthy adults (25 females, mean age: 33.6 y, age range 21–67 y) who underwent an fMRI session with hypercapnic blocs following a CO<sub>2</sub> inhalation protocol as in<sup>4</sup>. The CO<sub>2</sub> concentration was recorded at the level of their mouth using SmartLab Data Acquisition System (Hans Rudolf, Kansas, USA). The global delay between the BOLD and CO<sub>2</sub> signals was approximately 10 s due to the length of the sampling line (6 meters). The full description of this dataset can be found in the Supplementary Information.

After BIDS conversion of the MRI data, preprocessing was done using fMRIPrep with ICA-AROMA flag and no other option. Physiological data from the SmartLab system were formatted according to the BIDS before



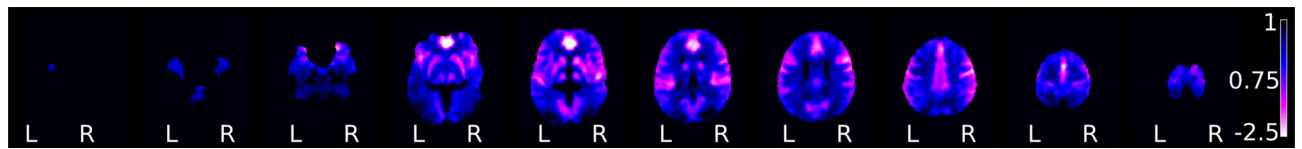


**Figure 4.** Effect of age on CVR for gray matter (GM) and white matter (WM). Data from the derivatives of CVRmap for 50 healthy participants acquired to validate the pipeline. The participants underwent CO<sub>2</sub> inhalation challenges using the protocol described in<sup>4</sup>. The straight lines correspond to the fitted models.

launching CVRmap. The pipeline finished without errors on the whole dataset and each individual reports have been visually inspected to ensure correct gas delivery and adequate etCO<sub>2</sub> timecourse estimation.

Two well-established features of CVR have been assessed on our dataset: (i) For a each subject, CVR in GM is larger than in WM and (ii) CVR in GM and WM both decrease with age. The method to extract the GM and WM masks is described in the fMRIPrep methods and is given as Supplementary Materials. The violin plot on Fig. 2 shows the CVR data from CVRmap grouped by age and are consistent with the literature<sup>10,21</sup>.

For each age group, mean CVR in GM was compared to mean CVR in WM using two-sample paired *t*-tests. In the three age groups, GM had significantly higher mean CVR than WM (all *p*-values lower than 0.001 %). As a complementary check, we linearly regressed GM and WM CVR means as a function of age (without grouping) and performed one-sample *t*-test on the fitted coefficients, see Fig. 4. For GM, the *r*-value  $r_{GM} = -0.37$  and the *p*-value  $p_{GM} = 0.8\%$ ; for WM, we found  $r_{WM} = -0.31$  and  $p_{WM} = 2.75\%$ ; we can therefore conclude that both these effects are significant at the conventional 5% *p*-value threshold.

For completeness, we also show on Fig. 5 the mean map of computed delays, which shows that GM is reached before WM, consistently with the literature<sup>10</sup>.

The dataset including raw data and derivatives is freely available online and can be used to test or compare other CVR computation methods, or can be used as a normative set to compare CVR of patients in research or clinical setups (Fig. 5).

### Comparison to other existing softwares

We have selected two other softwares to compare CVRmap: SeeVR<sup>29,30</sup> and MRICloud<sup>31</sup>. SeeVR is opensource and written in MATLAB. It contains a wide range of tools to handle, explore and analyze CVR or, more generally, various hemodynamic aspects of fMRI data. Thanks to tutorial scripts, users can create their own pipelines to explore their data and optimize each step of the processing. It is designed to work with physiological recordings from a RespirAct system (Thornhill Medical, Toronto, Canada). MRICloud is a cloud-based service on which users can upload their data. The pipeline is described in<sup>31</sup> but the exact implementation is not openly accessible. Apart from the anatomical and BOLD scan, there is no need (nor any possibility) to specify other parameters. Processing times are similar for the three softwares.

Both extremes come with their own benefits and disadvantages: the cost of SeeVR flexibility is that users need to have good scripting abilities to write their pipelines, but allow for potentially much more analyzes than CVRmap. MRICloud is very user-friendly but there is absolutely no freedom nor control on the processing. Moreover, as a web-based tool, its availability to users depends on the operational status of the servers and the associated computing clusters.

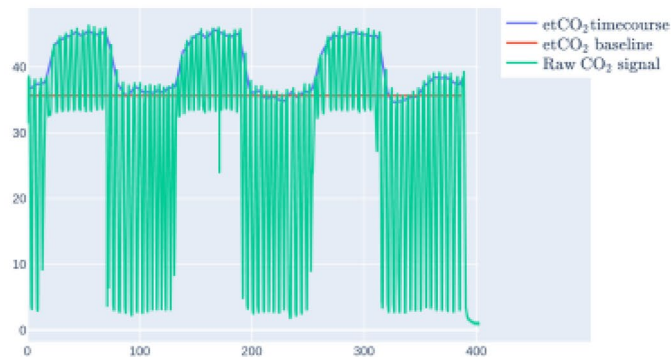
A summary of the distinctive features of SeeVR, MRICloud and CVRmap is presented in Table 1.

## Summary

- Subject ID: 001
- Functional Task: gas
- Output space(s): MNI152NLin2009cAsym
- CVRmap version: 2.0.20
- Command line options: ['analysis\_level': 'participant', 'participant\_label': '001', 'skip\_bids\_validator': False, 'sloppy': False, 'use\_aroma': False, 'overwrite': False, 'vesselsignal': False, 'globalsignal': False]

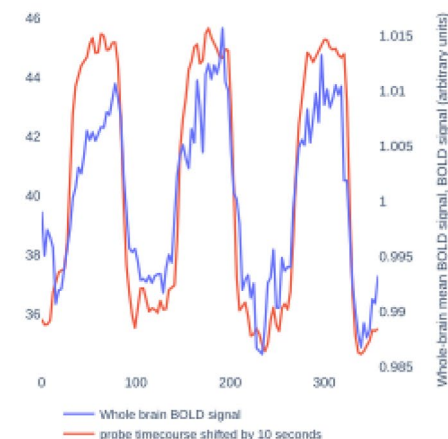
## Physiological

This graph shows the original breathing data with the reconstructed upper envelope and corresponding (units are mmmHg) baseline.



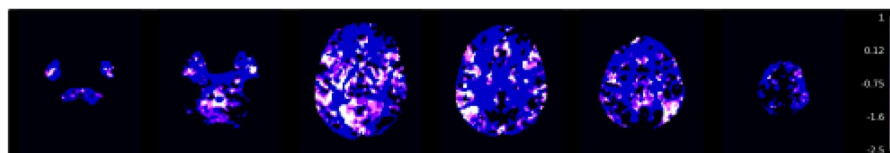
## etCO<sub>2</sub> versus Global BOLD signal

This graph shows the estimated etCO<sub>2</sub> (in mmmHg) and the global BOLD signal (arbitrary units).



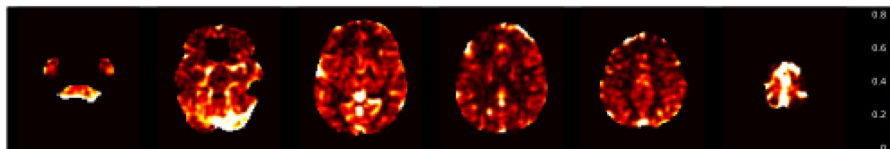
## Delay maps

Estimated delays (seconds), with the convention that zero delay corresponds to etCO<sub>2</sub> synchronized with global BOLD signal.



## Cerebrovascular Reactivity

Estimated CVR (units are % of BOLD signal variation/mmHg)



## Info on denoising

### Informations on denoising

- Noise regressors as classified by AROMA: [7, '9', '10', '12', '13', '14', '16', '17', '18', '19', '21', '22', '23', '25]
- Noise regressors after discarding regressors correlated with probe: [7, '9', '10', '12', '13', '14', '16', '17', '18', '19', '21', '22', '23', '25]
- CVR maps where smoothed with fwhm of (0=no smoothing): 5 mm

**Figure 5.** Mean of delay maps in normative dataset, in template (MNI) space and corrected for age (units: seconds). The delays are shifted as explained in the main text to set the global signal delay to zero. White and light purple-colored regions are reached before blue and darker ones. Displayed using the neurological convention.

	SeeVR	MRICloud	CVRmap
BIDS application	No	No	Yes
Opensource	Yes	No	Yes
Requires scripting	Yes	No	No
License	GPL3	Closed source	AGPL3
Containerized solution	No	No	Yes
Spatial smoothing	Optional	8 mm FWHM	Optional
Denoising	Flexible	Motion parameters	ICA-AROMA based
Graphical User Interface	No	Yes (web-based)	No

**Table 1.** Comparison of CVRmap to SeeVR and MRICloud.

## Summary

CVRmap is a specialized fMRI data processing program to compute maps of Cerebrovascular Reactivity complying with the BIDS standards. By sharing the code as well as a normative dataset of healthy participants, our goal is to offer to the community a standard framework for the study of CVR in potentially any relevant research topic, whether in clinical or more neuroscience-oriented projects. With this effort, we push the field to be part of the openscience culture, fostering the transparency of the methods, collaborative work and data sharing. Having such tools appears to be crucial given the quickly increasing applications of CVR.

## Ethical approval

The research protocol was approved by the CUB Hôpital Erasme Ethics Committee. Written informed consent was obtained from all participants prior to their participation. They were compensated monetarily for the loss of working hours and travel expenses.

## Data availability

Raw, preprocessed and processed data from the normative dataset are available on openneuro<sup>32</sup> under the Creative Commons license. All anatomical scans have been defaced using pydeface<sup>33</sup>.

## Code availability

CVRmap is available under the AGPLv3 license at <https://github.com/ln2t/cvrmap>. Docker images corresponding to every new release are made available on Docker Hub. The GitHub repository also contain instructions to preprocess the data using fMRIPrep providing sample commands to be adapted for any dataset. Commands used to analyze the data are included in the readme file. The code, used to generate the figures in the present paper from the openly accessible dataset, is shared in the form of a jupyter notebook at <https://github.com/ln2t/cvrmap-paper>. This script also serves as an example of how a group-level analysis can be easily designed from the processed individual data, and contain the two-sample paired *t*-tests comparing CVR in GM and WM in each age group. The data denoising included in CVRmap uses tools from the FMRIB Software Library (FSL, Release 6.0 (c) 2018, The University of Oxford). The CVRmap version used to process the data presented in this manuscript is 2.0.19, and fMRIPrep preprocessing was done using v21.0.4.

Received: 7 November 2023; Accepted: 19 March 2024

Published online: 27 March 2024

## References

- Grubb, R. L., Raichle, M. E., Eichling, J. O. & Ter-Pogossian, M. M. The effects of changes in PaCO<sub>2</sub> on cerebral blood volume, blood flow, and vascular mean transit time. *Stroke* **5**, 630–639. <https://doi.org/10.1161/01.str.5.5.630> (1974).
- Chen, J. J. & Pike, G. B. BOLD-specific cerebral blood volume and blood flow changes during neuronal activation in humans. *NMR Biomed.* **22**, 1054–1062. <https://doi.org/10.1002/nbm.1411> (2009).
- Leung, T. S. *et al.* Estimating a modified Grubb's exponent in healthy human brains with near infrared spectroscopy and transcranial Doppler. *Physiol. Meas.* **30**, 1–12. <https://doi.org/10.1088/0967-3334/30/1/001> (2009).
- Lu, H. *et al.* MRI mapping of cerebrovascular reactivity via gas inhalation challenges. *J. Vis. Exp.* 52306, 10.3791/52306 (2014). 0/0.
- Urbach, A. L., MacIntosh, B. J. & Goldstein, B. I. Cerebrovascular reactivity measured by functional magnetic resonance imaging during breath-hold challenge: A systematic review. *Neurosci. Biobehav. Rev.* **79**, 27–47. <https://doi.org/10.1016/j.neubiorev.2017.05.003> (2017).
- Bhagal, A. A. *et al.* Examining the regional and cerebral depth-dependent BOLD cerebrovascular reactivity response at 7 T. *NeuroImage* **114**, 239–248. <https://doi.org/10.1016/j.neuroimage.2015.04.014> (2015). 9/0.
- Wise, R. G. *et al.* Dynamic forcing of end-tidal carbon dioxide and oxygen applied to functional magnetic resonance imaging. *J. Cereb. Blood Flow Metab.* **27**, 1521–1532. <https://doi.org/10.1038/sj.jcbfm.9600465> (2007). 4/0.
- Pinto, J., Bright, M., Bulte, D. & Figueiredo, P. Cerebrovascular reactivity mapping without gas challenges: A methodological guide. *Front. Physiol.* <https://doi.org/10.3389/fphys.2020.608475> (2021).
- Poublanc, J. *et al.* Measuring cerebrovascular reactivity: The dynamic response to a step hypercapnic stimulus. *J. Cereb. Blood Flow Metab. Off. J. Int. Soc. Cereb. Blood Flow Metab.* **35**, 1746–1756. <https://doi.org/10.1038/jcbfm.2015.114> (2015).
- Sleight, E., Stringer, M. S., Marshall, I., Wardlaw, J. M. & Thrippleton, M. J. Cerebrovascular reactivity measurement using magnetic resonance imaging: A systematic review. *Front. Physiol.* <https://doi.org/10.3389/fphys.2021.643468> (2021).



11. Agarwal, S., Sair, H. I. & Pillai, J. J. The problem of neurovascular uncoupling. *Neuroimaging Clin. N. Am.* **31**, 53–67. <https://doi.org/10.1016/j.nic.2020.09.003> (2021).
12. Pillai, J. J. & Mikulis, D. J. Cerebrovascular reactivity mapping: An evolving standard for clinical functional imaging. *Am. J. Neuroradiol.* **36**, 7–13. <https://doi.org/10.3174/ajnr.A3941> (2015).
13. Gorgolewski, K. J. *et al.* The brain imaging data structure, a format for organizing and describing outputs of neuroimaging experiments. *Sci. Data* **3**, 160044. <https://doi.org/10.1038/sdata.2016.44> (2016). Number: 1 Publisher: Nature Publishing Group.
14. Esteban, O. *et al.* fMRIPrep: A robust preprocessing pipeline for functional MRI. *Nat. Methods* **16**, 111–116. <https://doi.org/10.1038/s41592-018-0235-4> (2019).
15. Pruim, R. H. R. *et al.* ICA-AROMA: A robust ICA-based strategy for removing motion artifacts from fMRI data. *NeuroImage* **112**, 267–277. <https://doi.org/10.1016/j.neuroimage.2015.02.064> (2015).
16. Moia, S. *et al.* ICA-based denoising strategies in breath-hold induced cerebrovascular reactivity mapping with multi echo BOLD fMRI. *NeuroImage* **233**, 117914. <https://doi.org/10.1016/j.neuroimage.2021.117914> (2021).
17. Piechnik, S. K., Chiarelli, P. A. & Jezzard, P. Modelling vascular reactivity to investigate the basis of the relationship between cerebral blood volume and flow under CO<sub>2</sub> manipulation. *NeuroImage* **39**, 107–118. <https://doi.org/10.1016/j.neuroimage.2007.08.022> (2008).
18. Tong, Y., Bergethon, P. R. & Frederick, B. d. An improved method for mapping cerebrovascular reserve using concurrent fMRI and near-infrared spectroscopy with Regressor Interpolation at Progressive Time Delays (RIPTiDe). *NeuroImage* **56**, 2047–2057. <https://doi.org/10.1016/j.neuroimage.2011.03.071> (2011). 6/0.
19. Donahue, M. J. *et al.* Time delay processing of hypercapnic fMRI allows quantitative parameterization of cerebrovascular reactivity and blood flow delays. *J. Cereb. Blood Flow Metab.* **36**, 1767–1779. <https://doi.org/10.1177/0271678X15608643> (2016). 8/22.
20. Erdoğan, S. B., Tong, Y., Hocke, L. M., Lindsey, K. P. & deB Frederick, B. Correcting for blood arrival time in global mean regression enhances functional connectivity analysis of resting state fMRI-BOLD signals. *Front. Hum. Neurosci.* **10**. <https://doi.org/10.3389/fnhum.2016.00311> (2016).
21. Lu, H. *et al.* Alterations in cerebral metabolic rate and blood supply across the adult lifespan. *Cereb. Cortex* **21**, 1426–1434. <https://doi.org/10.1093/cercor/bhq224> (2011).
22. Esteban, O. *et al.* Analysis of task-based functional MRI data preprocessed with fMRIPrep. bioRxiv 694364. <https://doi.org/10.1101/694364> (2019).
23. Liu, P., De Vis, J. B. & Lu, H. Cerebrovascular reactivity (CVR) MRI with CO<sub>2</sub> challenge: A technical review. *NeuroImage* **187**, 104–115. <https://doi.org/10.1016/j.neuroimage.2018.03.047> (2019).
24. Cohen, A. D. & Wang, Y. Improving the assessment of breath-holding induced cerebral vascular reactivity using a multiband multi-echo ASL/BOLD sequence. *Sci. Rep.* **9**, 5079. <https://doi.org/10.1038/s41598-019-41199-w> (2019). Publisher: Nature Publishing Group.
25. Cohen, A. D. *et al.* Improving the breath-holding CVR measurement using the multiband multi-echo EPI sequence. *Front. Physiol.* **12**, 619714. <https://doi.org/10.3389/fphys.2021.619714> (2021).
26. Community, T. t. *et al.* ME-ICA/tedana: 23.0.1. <https://doi.org/10.5281/zenodo.7926293> (2023).
27. Champagne, A. A., Bhogal, A. A., Coverdale, N. S., Mark, C. I. & Cook, D. J. A novel perspective to calibrate temporal delays in cerebrovascular reactivity using hypercapnic and hyperoxic respiratory challenges. *NeuroImage* **187**, 154–165. <https://doi.org/10.1016/j.neuroimage.2017.11.044> (2019). 19/0.
28. Frederick, B. d., Nickerson, L. D. & Tong, Y. Physiological denoising of BOLD fMRI data using Regressor Interpolation at Progressive Time Delays (RIPTiDe) processing of concurrent fMRI and near-infrared spectroscopy (NIRS). *NeuroImage* **60**, 1913–1923. <https://doi.org/10.1016/j.neuroimage.2012.01.140> (2012). 6/0.
29. Bhogal, A. A. *abhogal-lab/seevr*. Zenodo <https://doi.org/10.5281/zenodo.6532362> (2022).
30. Bhogal, A. A. Medullary vein architecture modulates the white matter BOLD cerebrovascular reactivity signal response to CO<sub>2</sub>: Observations from high-resolution T2\* weighted imaging at 7T. *NeuroImage* **245**, 118771. <https://doi.org/10.1016/j.neuroimage.2021.118771> (2021).
31. Liu, P. *et al.* CVR-MRICloud: An online processing tool for CO<sub>2</sub>-inhalation and resting-state cerebrovascular reactivity (CVR) MRI data. *PLoS ONE* **17**, e0274220. <https://doi.org/10.1371/journal.pone.0274220> (2022).
32. Rovai, A., Lolli, V., Trotta, N., Goldman, S. & De Tiege, X. cerebrovascular reactivity normative dataset. *OpenNeuro* <https://doi.org/10.18112/openneuro.ds004604.v1.1.0> (2023).
33. Gorgolewski, C. *et al.* cbinyu/pydeface: v2.0.6. Zenodo. 10.5281/zenodo.5838619 (2022)

## Acknowledgements

We would like to thank Dante Mantini for discussions at the early stage of this project. VL has been supported by *Fond Erasme* (Brussels, Belgium). XDT is a clinical researcher at *Fond de la Recherche Scientifique* (FRS-FNRS, Brussels, Belgium). This study has been supported by a research grant from the *Fond Erasme* (“AVN research convention”). The PET-MR project at the *Hôpital Universitaire de Bruxelles* is financially supported by the *Association Vinçotte Nuclear* (AVN, Brussels, Belgium).

## Author contributions

A.R., L.V., X.D.T. and S.G. designed the study. A.R. developed CVRmap including code writing, testing, documentation and processed the normative dataset. V.L., N.T. and A.R. acquired and curated the data. A.R., N.T., S.G. and X.D.T. assisted with writing and editing the manuscript. S.G. and X.D.T. obtained funding.

## Competing interests

The authors declare no competing interests.

## Additional information

**Supplementary Information** The online version contains supplementary material available at <https://doi.org/10.1038/s41598-024-57572-3>.

**Correspondence** and requests for materials should be addressed to A.R.

**Reprints and permissions information** is available at [www.nature.com/reprints](http://www.nature.com/reprints).

**Publisher’s note** Springer Nature remains neutral with regard to jurisdictional claims in published maps and institutional affiliations.



**Open Access** This article is licensed under a Creative Commons Attribution 4.0 International License, which permits use, sharing, adaptation, distribution and reproduction in any medium or format, as long as you give appropriate credit to the original author(s) and the source, provide a link to the Creative Commons licence, and indicate if changes were made. The images or other third party material in this article are included in the article's Creative Commons licence, unless indicated otherwise in a credit line to the material. If material is not included in the article's Creative Commons licence and your intended use is not permitted by statutory regulation or exceeds the permitted use, you will need to obtain permission directly from the copyright holder. To view a copy of this licence, visit <http://creativecommons.org/licenses/by/4.0/>.

© The Author(s) 2024